

Humidity Effects on PFPE Lubricant Bonding to a-CH_x Overcoats

Ryan Z. Lei and Andrew J. Gellman*

Department of Chemical Engineering, Carnegie Mellon University,
Pittsburgh, Pennsylvania 15213

Received December 7, 1999. In Final Form: May 23, 2000

The continued reduction in the head–disk separation of magnetic data storage systems and the corresponding increase in the frequency of head–disk contacts will place severe stress on the lubricant and overcoat used to protect the surfaces of magnetic media. With decreasing fly heights, environmental conditions such as temperature and humidity that influence the lubricant–overcoat interactions become increasingly important to the tribological performance of the head–disk interface. It is essential to obtain a fundamental understanding of the molecular interactions at the lubricant–overcoat interface in order to maintain the reliability of future hard disk drives. The coadsorption of model fluoro alcohols and fluoro ethers with water was studied to gain a fundamental understanding of the effects of humidity on the bonding of perfluoropolyalkyl ether (PFPE) lubricants to amorphous hydrogenated carbon (a-CH_x) overcoats. Temperature-programmed desorption experiments were performed using 2,2,2-trifluoroethanol (CF₃CH₂-OH) coadsorbed with water and perfluorodiethyl ether [(CF₃CF₂)₂O] coadsorbed with water. The results indicate that the presence of water increases the desorption energy of CF₃CH₂OH on the a-CH_x overcoat but decreases the desorption energy of (CF₃CF₂)₂O on a-CH_x overcoats. The implication of these results is that there is a net increase in the mobility of PFPE lubricant films when exposed to humid environments.

1. Introduction

Magnetic hard disks will serve as the primary data storage technology in computers for years to come.¹ This technology uses a 150–300 Å layer of magnetic material deposited on the hard disk as the medium for data storage. Data are written to and read from the magnetic film by a small recording head that flies over the surface of the disk as it spins. A 100–200 Å thick hydrogenated or nitrogenated amorphous carbon overcoat² (a-CH_x and a-CN_x, respectively) is sputtered onto the magnetic film to protect it from damage due to contacts between the head and disk surface. For additional protection, a 5–20 Å layer of perfluoropolyalkyl ether (PFPE) lubricant^{2–4} is applied to the surface of the amorphous carbon overcoat. The recording head flies over the disk surface and lubricant film on a layer of air less than 500 Å thick.^{2,5} Since 1991, the areal recording density (the number of bits stored per unit area) has maintained a growth rate of 60% per year.⁶ To continue this growth rate, the gap between the recording head and the disk surface must be decreased continuously. Ultimately there will only be room for a few atomic and molecular layers of overcoat and lubricant to protect the magnetic media from contact with the head. With such small head-to-disk spacing, a fundamental understanding of the molecular interactions at the head–disk interface is essential for optimizing data protection and thus increasing storage density.

As head fly heights continue to decrease, environmental conditions such as temperature and humidity that influ-

ence the lubricant–overcoat interactions become increasingly important to the tribological properties of the head–disk interface. Many studies have been conducted to investigate the effects of humidity on head–disk tribological performance.^{7–13} Dai et al.⁷ investigated the effect of humidity on the spatial distribution of perfluorinated lubricants on hard carbon overcoats. The technique used was noncontact atomic force microscopy, capable of generating nanometer resolution images of soft materials and liquid surfaces. They observed a general enhancement of lubricant mobility in the presence of water. In another study using drag and CSS (contact start and stop) tests, Zhao and Bhushan⁸ concluded that the durability of lubricated disks was lower at high humidity for all degrees of chemically bonded lubricant films. The consensus of these studies is that there is a general enhancement of PFPE mobility on a-CH_x films in humid environments. Some mobility of PFPE lubricants is desired for replenishment of areas depleted of lubricant by head–disk contacts, however, excess mobility will lead to lubricant spin-off decreasing the durability of the hard disk.

The aforementioned studies are macroscopic studies of the effect of humidity on the lubricant–overcoat interaction. The goal of our investigation is to approach this problem at a molecular level, trying to obtain a fundamental understanding of the molecular interactions between water, lubricant, and overcoat. The industry standard PFPE lubricant is Fomblin Zdol [HO–CH₂CF₂–(OC₂F₄)_{*n*}–

* To whom correspondence should be addressed.

(1) Simonds, J. L. *Phys. Today* **1995**, *48*, 26–32.

(2) Gellman, A. J. *Curr. Opin. Colloid Interface Sci.* **1998**, *3*, 368–372.

(3) Coffey, K. R.; Raman, V.; Staud, N.; Pocker, D. J. *IEEE Trans. Magn.* **1994**, *30*, 4146–4148.

(4) O'Conner, T. M.; Back, Y. R.; Jhon, M. S.; Min, B. G.; Yoon, D. Y.; Karis, T. E. *J. Appl. Phys.* **1996**, *79*, 5788–5790.

(5) Mate, C. M.; Homola, A. M. *Molecular Tribology of Disk Drives*; Bhushan, B., Ed.; Kluwer Academic Publishers: Netherlands, 1997; pp 647–661.

(6) Kryder, M. H. *Mater. Res. Soc. Bull.* **1996**, *9*, 17–19.

(7) Dai, Q.; Vurens, G. *Langmuir* **1997**, *13*, 4401–4406.

(8) Zhao, Z.; Bhushan, B. *Proc. Inst. Mech. Eng. Part J: J. Eng. Tribol.* **1997**, *211*, 295–301.

(9) Perry, S. S.; Somorjai, G. A.; Mate, C. M.; White, R. *Tribol. Lett.* **1995**, *1*, 47–58.

(10) Strom, B. D.; Bogy, D. B.; Bhatia, C. S.; Bhushan, B. *J. Tribol.* **1991**, *113*, 689–693.

(11) Yang, M.; Talke, F. E. *Effects of Gas Composition, Humidity and Temperature on the Tribology of the Head/Disk Interface—Part II: Model and Analysis*; STLE Preprint: Kissimmee, FL, 1995; Vol. No. 95-TC-6B-2.

(12) Binggeli, M.; Mate, C. M. *J. Vacuum Sci. Technol. B* **1995**, *13*, 1312–1315.

(13) Tian, H.; Matsudaira, T. *J. Tribol.* **1993**, *115*, 28–35.

(OCF₂)_m-OCF₂CH₂-OH], the structure of which consists of an ether-like backbone with hydroxyl end groups. Since Fomblin Zdol decomposes rather than desorb molecularly when heated on a hard disk surface, it is not possible to obtain molecular desorption spectra of Fomblin Zdol directly.^{9,14} Instead, (CF₃CF₂)₂O was used to model its ether-like backbone and CF₃CH₂OH to model its hydroxyl end groups. To study the effects of humidity on Zdol bonding to a-CH_x films, temperature-programmed desorption (TPD) spectra were obtained of perfluorodiethyl ether [(CF₃CF₂)₂O] coadsorbed with water and 2,2,2-trifluoroethanol [CF₃CH₂OH] coadsorbed with water on a-CH_x films.

The bonding mechanism of fluoroethers and fluoroalcohols to amorphous carbon overcoats has been examined in prior work. Cornaglia and Gellman conducted a study of the bonding of lubricants to a-CH_x overcoats by using small fluorocarbon ethers and their hydrogenated analogues.¹⁵ They concluded that ethers interact with a-CH_x surfaces through electron donation from the oxygen lone pairs, also known as dative bonding. This same model has been proposed for the bonding of ethers to several metal surfaces.^{16–21} Paserba et al. investigated the surface chemistry of fluoroethers and fluoroalcohols adsorbed on a-CN_x films and concluded that alcohols interact with these surfaces through hydrogen bonding.²²

The focus of the study described in this paper was to determine the effect of humidity on the dative bond of fluoroethers and the hydrogen bond of fluoroalcohols. We studied the coadsorption of water with (CF₃CF₂)₂O and CF₃CH₂OH on a-CH_x-coated disks obtained from Quantum Corp. and Seagate Corp. Temperature-programmed desorption experiments show that the desorption energy of (CF₃CF₂)₂O decreases with increasing water coverage on both the Quantum and Seagate disks. The desorption energy of CF₃CH₂OH increases with increasing water coverage on the Quantum disks. The results of this work are consistent with the increase in PFPE mobility on disk surfaces that has been observed in the presence of humidity.

2. Experimental Section

All experiments were performed in an ultrahigh vacuum (UHV) chamber with a base pressure of $<1 \times 10^{-10}$ Torr achieved through use of a cryopump and titanium sublimation pump. The chamber is equipped with two leak valves fitted with a stainless steel dosing tube. One of the leak valves is used to introduce vapor of the model lubricants [CF₃CH₂OH or (CF₃CF₂)₂O] into the chamber, while the other is used to introduce water vapor into the chamber. The chamber is also equipped with an Ametek Dycor quadrupole mass spectrometer (QMS), which has a mass range of 1–200 amu and is capable of monitoring up to eight masses simultaneously during TPD experiments.

Quantum Corp. and Seagate Corp. supplied magnetic hard disk platters sputter coated with a protective a-CH_x overcoat and no lubricant. The Seagate disks, denoted by a-CH_{Seag}, were sputtered in a 15% H₂ atmosphere. The atmospheric H₂ content

for the Quantum disks (a-CH_{Quan}) is unknown. Previous work with these types of films has shown that the fundamental nature of alcohol and ether adsorption on their surfaces is not influenced by subtle differences between films obtained from different sources.^{15,22} The disk platters were machine-punched to produce ~12.5 mm diameter samples for use in the UHV chamber. Two tantalum wires were spot-welded to the edge of the sample and mounted to a sample holder at the end of a manipulator. Once mounted to the manipulator, the disk sample could be cooled to ~100 K through contact with a liquid nitrogen reservoir and heated resistively at a constant rate to the melting point of aluminum. The sample temperature was measured using a chromel–alumel thermocouple spot-welded to the rear face of the sample.

The disk samples were used as received for the TPD experiments. Once inside the chamber the only cleaning consisted of simply heating to 400 K to induce desorption of adsorbed species such as water. The TPD spectra obtained during this initial heating did not reveal any desorption. This is not surprising since to achieve UHV conditions the sample was subjected to a bakeout in a vacuum for ~12 h. at roughly 450 K. Following this initial treatment, the condition of the surface, as determined by water, (CF₃CF₂)₂O, and CF₃CH₂OH adsorption and desorption, was highly reproducible. Irreversible changes such as dehydrogenation that do influence adsorbate desorption spectra only occur when the a-CH_x overcoats are heated to temperatures in excess of 500 K.¹⁵

The water used in this investigation was obtained from an in-house water purifier. The perfluorodiethyl ether [(CF₃CF₂)₂O, 90+%) was purchased from Stem Chemicals. The 2,2,2-trifluoroethanol [CF₃CH₂OH, 99.5%] was purchased from Lancaster Chemicals. All compounds were further purified before use through a series of freeze–pump–thaw cycles intended to remove any high vapor pressure contaminants.

Within the UHV chamber the sample was positioned adjacent to the stainless steel dosing tube and approximately 1 cm from an aperture to the QMS. The procedure for TPD experiments consisted of three steps: adsorption, desorption, and detection. The adsorption step entailed cooling the disk sample to <100 K and exposing its surface to either the (CF₃CF₂)₂O or the CF₃-CH₂OH and then to water at pressures ranging from 10^{–9} to 10^{–8} Torr for periods of 30–200 s. The exposures are reported in units of Langmuirs (1 Langmuir = 10^{–6} Torr s). To investigate any effects of the order of exposure, experiments were also conducted by adsorbing water first and then either (CF₃CF₂)₂O or CF₃-CH₂OH. Desorption involved heating the sample at a constant rate of 2 K/s from 100 to 400 K to induce the desorption of the adsorbed molecules. During heating, the QMS monitored the desorbing species and any decomposition products. The desorption peak temperatures were determined by fitting the top 10% of the peak using a Gaussian function. In all cases, adsorption and desorption of (CF₃CF₂)₂O, CF₃CH₂OH, and water were molecular and reversible with no indication of decomposition.

3. Results

3.1. CF₃CH₂OH, (CF₃CF₂)₂O, and H₂O on a-CH_x Individually. Before studying the coadsorption of species, we first examined the adsorption of CF₃CH₂OH, (CF₃-CF₂)₂O, and H₂O individually on a-CH_x. CF₃CH₂OH was chosen to model the hydroxyl end groups present in Fomblin Zdol. TPD spectra can be used to estimate interaction strengths of CF₃CH₂OH with a-CH_x films. Figure 1 shows TPD spectra of CF₃CH₂OH adsorbed at 100 K on the a-CH_{Quan} film. The spectra were generated by using the QMS to monitor $m/q = 31$ (CH₂OH⁺), the most intense ion in the fragmentation pattern of CF₃-CH₂OH, as a function of temperature during heating at 2 K/s. One additional mass-to-charge ratio of $m/q = 69$ (CF₃⁺) was monitored in order to detect the desorption of any decomposition products. No decomposition of CF₃-CH₂OH was observed. At the lowest coverage the adsorbed CF₃CH₂OH desorbs with a maximum rate at 196 K. As the exposure is increased, the desorption peak amplitude increases and shifts to lower temperatures until the

(14) Helmick, L. S.; Jones, W. R., Jr *NASA Technol. Memor.* **1990**, 102–493.

(15) Cornaglia, L.; Gellman, A. J. *J. Vacuum Sci. Technol. A* **1997**, *15*, 2755–2765.

(16) Meyers, J. M.; Gellman, A. J. *Surf. Sci.* **1997**, *372*, 171–178.

(17) Meyers, J. M.; Street, S. C.; Thompson, S.; Gellman, A. J. *Langmuir* **1996**, *12*, 1511–1519.

(18) Meyers, J. M.; Gellman, A. J. *Tribol. Lett.* **1996**, *2*, 47–55.

(19) Walczak, M. M.; Leavitt, P. K.; Thiel, P. A. *J. Am. Chem. Soc.* **1987**, *109*, 5621–5627.

(20) Walczak, M. M.; Thiel, P. A. *Surf. Sci.* **1989**, *224*, 425–450.

(21) Walczak, M. M.; Leavitt, P. K.; Thiel, P. A. *Tribol. Trans.* **1990**, *33*, 557–562.

(22) Paserba, K.; Shukla, N.; Gellman, A. J.; Gui, J.; Marchon, B. *Langmuir* **1999**, *15*, 1709–1715.

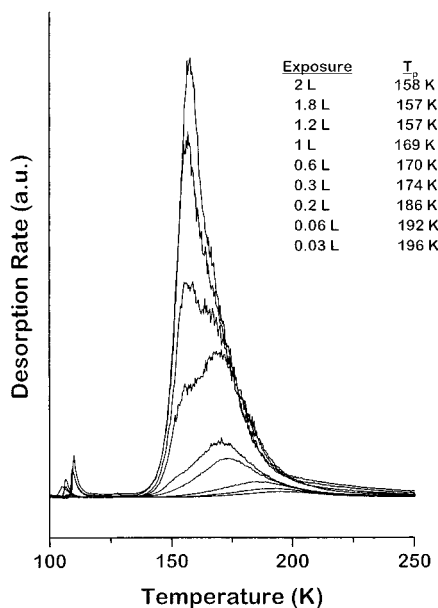


Figure 1. TPD spectra of $\text{CF}_3\text{CH}_2\text{OH}$ obtained as a function of exposure following adsorption on an $\text{a-CH}_{\text{Quan}}$ surface at 100 K. The spectra were generated by monitoring $m/q = 31$ ($\text{CH}_2\text{-OH}^+$). The heating rate was 2 K/s.

monolayer is saturated. Following monolayer saturation, a desorption peak appears at 157 K that does not saturate with increasing coverage and displays zero-order kinetics, indicative of bulk sublimation of multilayers. For the purposes of this work the definition of one monolayer coverage is the lowest coverage at which zero-order desorption kinetics are observed. Zero-order desorption manifests itself as overlap in the initial desorption rates and alignment of the low-temperature leading edges of the desorption curves. The multilayer peak desorption temperature is consistent with values found for $\text{CF}_3\text{CH}_2\text{-OH}$ adsorbed on a-CN_x films (159 K),²² $\text{Cu}(111)$ (165 K),²³ and ZrO_2 films (155 K).²⁴ The fundamental observation is that $\text{CF}_3\text{CH}_2\text{OH}$ adsorbs reversibly on the $\text{a-CH}_{\text{Quan}}$ film and desorbs with a peak desorption temperature that decreases with increasing coverage.

The $(\text{CF}_3\text{CF}_2)_2\text{O}$ was chosen as a model for the perfluoropolyether backbone of Fomblin Zdol. Figure 2 shows TPD spectra of $(\text{CF}_3\text{CF}_2)_2\text{O}$ adsorbed at 100 K on the $\text{a-CH}_{\text{Quan}}$ film. The spectra were generated by monitoring $m/q = 69$ (CF_3^+), as a function of temperature during heating at 2 K/s. Two additional mass-to-charge ratios of $m/q = 50$ (CF_2^+) and $m/q = 31$ (CF^+) were monitored in order to detect the desorption of any decomposition products. No decomposition of $(\text{CF}_3\text{CF}_2)_2\text{O}$ was observed. At the lowest coverage the adsorbed $(\text{CF}_3\text{CF}_2)_2\text{O}$ desorbs with a maximum rate at 180 K. The multilayer peak desorption temperature is 115 K and is consistent with values found for $(\text{CF}_3\text{CF}_2)_2\text{O}$ adsorbed on a-CH_x (113 K),¹⁵ a-CN_x films (118 K),²² $\text{Al}(110)$ (111 K),¹⁶ $\text{Cu}(111)$ (122 K),¹⁷ and ZrO_2 (125 K).²⁴ As in the case of $\text{CF}_3\text{CH}_2\text{OH}$, the fundamental observation for $(\text{CF}_3\text{CF}_2)_2\text{O}$ is that it adsorbs reversibly on the $\text{a-CH}_{\text{Quan}}$ film and its desorption peak temperature decreases with increasing coverage.

Water adsorption onto the a-CH_x films was used to simulate the effects of humidity. Figure 3 shows TPD spectra of water adsorbed at 100 K on the $\text{a-CH}_{\text{Quan}}$ film. The spectra were generated by monitoring $m/q = 18$

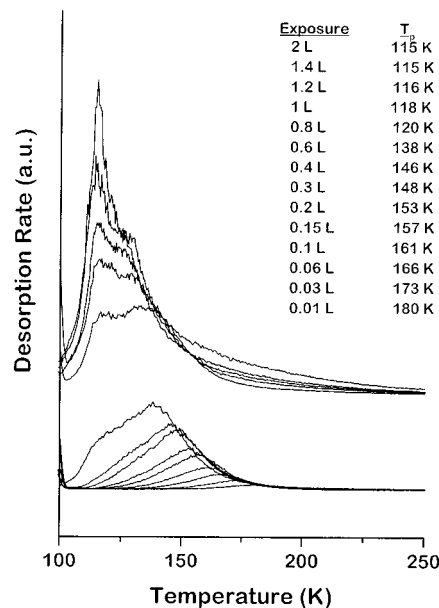


Figure 2. TPD spectra of $(\text{CF}_3\text{CF}_2)_2\text{O}$ obtained as a function of exposure following adsorption on an $\text{a-CH}_{\text{Quan}}$ surface at 100 K. The spectra were generated by monitoring $m/q = 69$ (CF_3^+). The heating rate was 2 K/s.

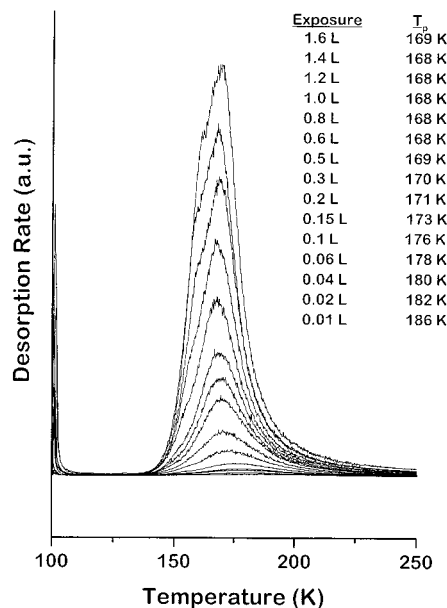


Figure 3. TPD spectra of water obtained as a function of exposure following adsorption on an $\text{a-CH}_{\text{Quan}}$ surface at 100 K. The spectra were generated by monitoring $m/q = 18$ (H_2O^+). The heating rate was 2 K/s.

(H_2O^+), as a function of temperature during heating at 2 K/s. At the lowest coverage the adsorbed water desorbs with a maximum rate at 186 K. The multilayer peak desorption temperature is 168 K and is consistent with values found for water adsorbed on $\text{Pt}(111)$ (165 K),²⁴ $\text{Ru}(0001)$ (155 K),²⁵ and $\text{Ru}(100)$ (160 K).²⁶ The range or spread of peak temperatures observed for H_2O desorption is much lower than for either $(\text{CF}_3\text{CF}_2)_2\text{O}$ or $\text{CF}_3\text{CH}_2\text{OH}$; however, the fundamental observation of reversible adsorption and desorption without reaction on the $\text{a-CH}_{\text{Quan}}$ film holds for all three species.

The exact conditions used for the preparation of a-CH_x films used in the data storage industry varies among

(23) McFadden, C. F.; Gellman, A. J. *Langmuir* **1995**, *11*, 273–280.

(24) Maurice, V.; Takeuchi, K.; Salmeron, M.; Somorjai, G. A. *Surf. Sci.* **1991**, *250*, 99–111.

(25) Doering, D. L.; Madey, T. E. *Surf. Sci.* **1982**, *123*, 305–337.

(26) Leavitt, P. K.; Thiel, P. A. *J. Vacuum Sci. Technol. A* **1989**, *8*, 2269–2273.

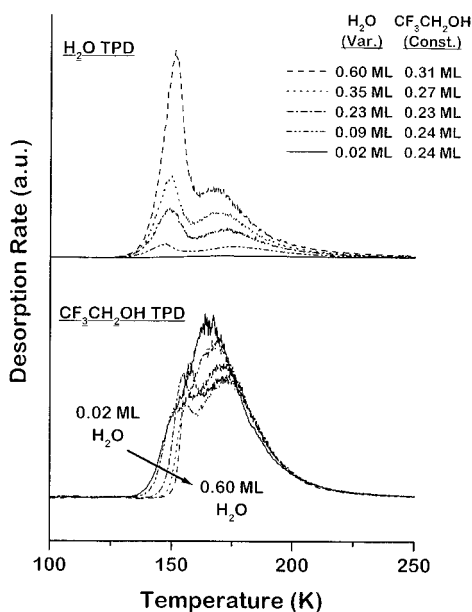


Figure 4. TPD spectra of coadsorbed $\text{CF}_3\text{CH}_2\text{OH}$ and water obtained as a function of coverage following adsorption on an $\text{a-CH}_{\text{Quan}}$ surface at 100 K. Each pair of spectra illustrated with a given line type in the top and bottom halves of the figure correspond to one experiment with a given coverage of H_2O (variable from 0.02 to 0.60 ML) coadsorbed with $\text{CF}_3\text{CH}_2\text{OH}$ (constant at 0.26 ± 0.03 ML). Examination of the low-temperature leading edge of the $\text{CF}_3\text{CH}_2\text{OH}$ spectra reveals that the desorption rate decreases with increasing water coverage. $\text{CF}_3\text{CH}_2\text{OH}$ was adsorbed onto the surface before the water. The spectra were generated by simultaneously monitoring $m/q = 31$ (CH_2OH^+) and $m/q = 18$ (H_2O^+) during heating at 2 K/s.

manufacturers. The objective of our program to study the surface chemistry and properties of these films has been to identify the chemical characteristics that are common to all films and independent of their source. To that end the experiments described above have also been performed on a-CH_x films provided by Seagate Corp. The desorption spectra of $(\text{CF}_3\text{CF}_2)_2\text{O}$, $\text{CF}_3\text{CH}_2\text{OH}$, and H_2O on the $\text{a-CH}_{\text{Quan}}$ film shown in Figures 1, 2, and 3, respectively, are all qualitatively similar to those obtained on the $\text{a-CH}_{\text{Seag}}$ films and on films obtained from other manufacturers and described in previous work.^{15,22} All three molecules adsorb reversibly without reacting and their desorption spectra reveal peaks that shift to lower temperatures with increasing coverage.

3.2. Coadsorption of Water and $\text{CF}_3\text{CH}_2\text{OH}$ on a-CH_x . The effects of humidity on the interaction of Fomblin Zdol end groups with a-CH_x films have been examined by studying the coadsorption of $\text{CF}_3\text{CH}_2\text{OH}$ with increasing coverages of water. Figure 4 shows the TPD spectra of coadsorbed $\text{CF}_3\text{CH}_2\text{OH}$ and water on the $\text{a-CH}_{\text{Quan}}$ overcoat. The order of adsorption onto the $\text{a-CH}_{\text{Quan}}$ overcoat was $\text{CF}_3\text{CH}_2\text{OH}$ followed by water, and both were exposed with the film held at 100 K. The $\text{CF}_3\text{CH}_2\text{OH}$ coverage was kept constant at 0.26 ± 0.03 ML while the water coverage ranged from 0.02 to 0.60 ML. In general we have tried to work with low adsorbate coverages; however, in the case of $\text{CF}_3\text{CH}_2\text{OH}$ it was difficult to reproducibly generate coverages lower than ~ 0.20 ML due to its slow pumping characteristics. The spectra were generated by simultaneously monitoring $m/q = 31$ (CH_2OH^+) and $m/q = 18$ (H_2O^+). Several additional mass-to-charge ratios were monitored to verify that the only species observed in the desorption spectra were water

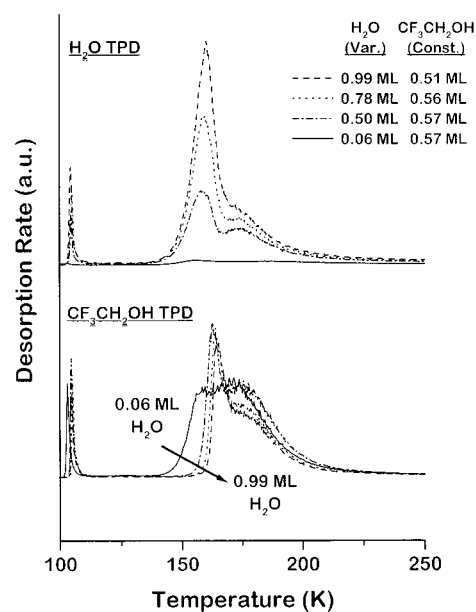


Figure 5. TPD spectra of coadsorbed $\text{CF}_3\text{CH}_2\text{OH}$ and water obtained as a function of coverage following adsorption on an $\text{a-CH}_{\text{Quan}}$ surface at 100 K. Each pair of spectra illustrated with a given line type in the top and bottom halves of the figure correspond to one experiment with a given coverage of H_2O (variable from 0.06 to 0.99 ML) coadsorbed with $\text{CF}_3\text{CH}_2\text{OH}$ (constant at 0.55 ± 0.03 ML). Examination of the low-temperature leading edge of the $\text{CF}_3\text{CH}_2\text{OH}$ spectra reveals that the desorption rate decreases with increasing water coverage. $\text{CF}_3\text{CH}_2\text{OH}$ was adsorbed onto the surface before the water. The spectra were generated by simultaneously monitoring $m/q = 31$ (CH_2OH^+) and $m/q = 18$ (H_2O^+) during heating at 2 K/s.

and $\text{CF}_3\text{CH}_2\text{OH}$ and there was no decomposition of adsorbates or reaction between them.

In looking at the spectra in Figure 4 it is important to remember that TPD measures the desorption rate at a given temperature. Interpretation of these spectra is complicated by several things. For one, the coverages vary throughout the temperature range of the desorption feature. However, at the low-temperature portion of the desorption features the $\text{CF}_3\text{CH}_2\text{OH}$ coverages are roughly constant and determined by the initial coverage. Second, Figures 1 and 3 reveal that water and $\text{CF}_3\text{CH}_2\text{OH}$ both desorb in the same temperature range and thus both coverages are changing at the same time. As a result of these complications we have chosen simply to examine the low-temperature leading edges of the spectra where the coverages of both species are fixed by the starting conditions. Examination of the $\text{CF}_3\text{CH}_2\text{OH}$ desorption spectra at a temperature of 150 K reveals that the desorption rate of $\text{CF}_3\text{CH}_2\text{OH}$ decreases with increasing water coverage.

The coadsorption of water and $\text{CF}_3\text{CH}_2\text{OH}$ was also studied at a higher constant $\text{CF}_3\text{CH}_2\text{OH}$ coverage of 0.55 ± 0.03 ML (roughly twice that of Figure 4). Figure 5 shows the TPD spectra of coadsorbed $\text{CF}_3\text{CH}_2\text{OH}$ at this higher coverage and water at a range of coverages. Examination of the $\text{CF}_3\text{CH}_2\text{OH}$ desorption peak at low temperatures reveals that the desorption rate decreases with increasing water coverage. This decrease in desorption rate with increasing water coverage implies an increase in desorption energy of $\text{CF}_3\text{CH}_2\text{OH}$ with increasing water coverage.

Although the primary focus of this work has been the effect of water on the adsorption of $\text{CF}_3\text{CH}_2\text{OH}$, it is important to note that at the same time $\text{CF}_3\text{CH}_2\text{OH}$ influences the desorption of water. This can be observed

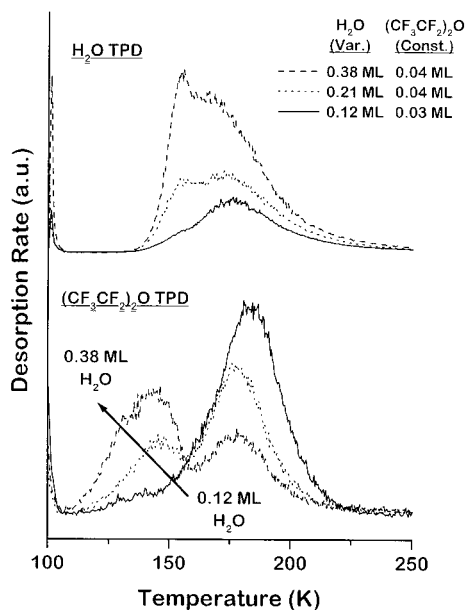


Figure 6. TPD spectra of coadsorbed $(\text{CF}_3\text{CF}_2)_2\text{O}$ and water obtained as a function of coverage following adsorption on an $\text{a-CH}_{\text{Quan}}$ surface at 100 K. Each pair of spectra illustrated with a given line type in the top and bottom halves of the figure correspond to one experiment with a given coverage of H_2O (variable from 0.12 to 0.38 ML) coadsorbed with $(\text{CF}_3\text{CF}_2)_2\text{O}$ (constant at 0.04 ± 0.004 ML). Examination of the low-temperature leading edge of the $(\text{CF}_3\text{CF}_2)_2\text{O}$ spectra reveals that the desorption rate increases with increasing water coverage. Water was adsorbed onto the surface before $(\text{CF}_3\text{CF}_2)_2\text{O}$. The spectra were generated by simultaneously monitoring $m/q = 69$ (CF_3^+) and $m/q = 18$ (H_2O^+) while heating at 2 K/s.

by comparing the desorption spectra of water in Figures 3–5. The fact that both water and $\text{CF}_3\text{CH}_2\text{OH}$ influence each other is a result of the fact that both desorb in roughly the same temperature range rather than one before the other.

The coadsorption of water and $\text{CF}_3\text{CH}_2\text{OH}$ on the $\text{a-CH}_{\text{Seag}}$ film has also been studied in order to compare to the results described above on the $\text{a-CH}_{\text{Quan}}$ film. Some features of the results clearly depend on the source of the film. The TPD spectra of coadsorbed water and $\text{CF}_3\text{CH}_2\text{OH}$ on $\text{a-CH}_{\text{Quan}}$ exhibit two peaks in the water desorption spectra, as shown in Figures 4 and 5. On the $\text{a-CH}_{\text{Seag}}$ film, however, the water desorbs in a single desorption feature such as that shown in Figure 3. The reduction in the $\text{CF}_3\text{CH}_2\text{OH}$ desorption rate as a result of coadsorption with water is only observed on the $\text{a-CH}_{\text{Seag}}$ film at $\text{CF}_3\text{CH}_2\text{OH}$ coverages of < 0.1 ML but not at higher coverages.

3.3. Coadsorption of Water and $(\text{CF}_3\text{CF}_2)_2\text{O}$ on a-CH_x . The effect of humidity on the interaction of the ether backbones of PFPE lubricants with a-CH_x films has been examined by studying the coadsorption of $(\text{CF}_3\text{CF}_2)_2\text{O}$ with water. Figure 6 shows TPD spectra of coadsorbed $(\text{CF}_3\text{CF}_2)_2\text{O}$ and water adsorbed on the $\text{a-CH}_{\text{Quan}}$ surface. The order of exposure was water first followed by $(\text{CF}_3\text{CF}_2)_2\text{O}$ with the $\text{a-CH}_{\text{Quan}}$ film held at 100 K. The $(\text{CF}_3\text{CF}_2)_2\text{O}$ coverage was kept constant at 0.04 ± 0.01 ML while the water coverage ranged from 0.12 to 0.38 ML. The spectra were generated by simultaneously monitoring $m/q = 69$ (CF_3^+) and $m/q = 18$ (H_2O^+). Several additional mass-to-charge ratios were monitored to verify that there was no decomposition or reaction between $(\text{CF}_3\text{CF}_2)_2\text{O}$ and water. As in the case of $\text{CF}_3\text{CH}_2\text{OH}$ coadsorption with water, there was no evidence of any reaction between the $(\text{CF}_3\text{CF}_2)_2\text{O}$ and the water.

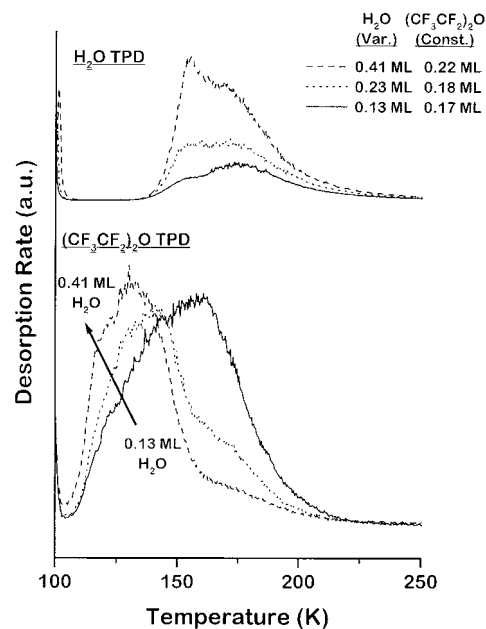


Figure 7. TPD spectra of coadsorbed $(\text{CF}_3\text{CF}_2)_2\text{O}$ and water obtained as a function of coverage following adsorption on an $\text{a-CH}_{\text{Quan}}$ surface at 100 K. Each pair of spectra illustrated with a given line type in the top and bottom halves of the figure correspond to one experiment with a given coverage of H_2O (variable from 0.13 to 0.41 ML) coadsorbed with $(\text{CF}_3\text{CF}_2)_2\text{O}$ (constant at 0.19 ± 0.03 ML). Examination of the low-temperature leading edge of the $(\text{CF}_3\text{CF}_2)_2\text{O}$ spectra reveals that the desorption rate increases with increasing water coverage. Water was adsorbed onto the surface before $(\text{CF}_3\text{CF}_2)_2\text{O}$. The spectra were generated by simultaneously monitoring $m/q = 69$ (CF_3^+) and $m/q = 18$ (H_2O^+) during heating at 2 K/s.

Analysis of the TPD spectra for coadsorbed $(\text{CF}_3\text{CF}_2)_2\text{O}$ and water is somewhat simpler than for coadsorbed $\text{CF}_3\text{CH}_2\text{OH}$ and water due to the fact that the desorption temperature ranges for the $(\text{CF}_3\text{CF}_2)_2\text{O}$ and water do not overlap to the same extent. As can be seen in Figures 2 and 3 the $(\text{CF}_3\text{CF}_2)_2\text{O}$ tends to desorb at lower temperatures than water with significant overlap only occurring at low $(\text{CF}_3\text{CF}_2)_2\text{O}$ coverages. Examination of the $(\text{CF}_3\text{CF}_2)_2\text{O}$ spectra in Figure 6 reveals a clear shift of the $(\text{CF}_3\text{CF}_2)_2\text{O}$ desorption peaks to lower temperatures as a result of the coadsorption of water. At 140 K, the desorption rate of $(\text{CF}_3\text{CF}_2)_2\text{O}$ clearly increases with increasing water coverage. This increase in desorption rate with increasing water coverage implies a decrease in the $(\text{CF}_3\text{CF}_2)_2\text{O}$ desorption energy as a result of the presence of the water.

Coadsorption experiments using $(\text{CF}_3\text{CF}_2)_2\text{O}$ and water were also conducted for higher constant $(\text{CF}_3\text{CF}_2)_2\text{O}$ coverage than in Figure 6. Figure 7 shows the TPD spectra of coadsorbed $(\text{CF}_3\text{CF}_2)_2\text{O}$ and water obtained with a water coverage ranging from 0.13 to 0.41 ML while the $(\text{CF}_3\text{CF}_2)_2\text{O}$ coverage was kept constant at 0.19 ± 0.03 ML. As in the lower coverage case, examination of the spectra at a low temperature (125 K) reveals that the $(\text{CF}_3\text{CF}_2)_2\text{O}$ desorption rate increases with increasing water coverage. This increase in desorption rate with increasing water coverage implies a decrease in the desorption energy of $(\text{CF}_3\text{CF}_2)_2\text{O}$ as a result of coadsorption with water.

To investigate the differences between a-CH_x films obtained from different sources, TPD of coadsorbed $(\text{CF}_3\text{CF}_2)_2\text{O}$ and water was studied on the $\text{a-CH}_{\text{Seag}}$ films. Although there are subtle differences in the TPD spectra obtained on the $\text{a-CH}_{\text{Seag}}$ and the $\text{a-CH}_{\text{Quan}}$ films, the basic observation that coadsorbed water increases the desorption rate of the $(\text{CF}_3\text{CF}_2)_2\text{O}$ was made on both surfaces.

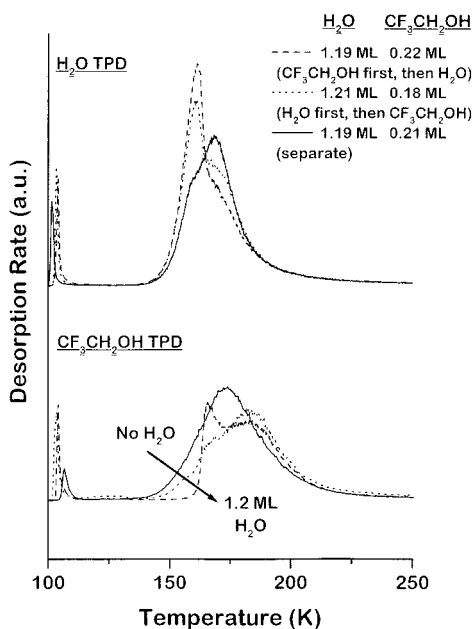


Figure 8. TPD spectra of coadsorbed $\text{CF}_3\text{CH}_2\text{OH}$ and water with different orders of exposure and TPD spectra of $\text{CF}_3\text{CH}_2\text{OH}$ and water adsorbed individually on an $\text{a-CH}_{\text{Quan}}$ surface at 100 K. Although the order of exposure influences the water and the $\text{CF}_3\text{CH}_2\text{OH}$ TPD spectra the presence of water decreases the initial rate of desorption at the low temperature leading edge of the $\text{CF}_3\text{CH}_2\text{OH}$ spectrum. The water coverage was kept constant at 1.20 ± 0.01 ML. The $\text{CF}_3\text{CH}_2\text{OH}$ coverage was kept constant at 0.20 ± 0.02 ML. The spectra were generated by simultaneously monitoring $m/q = 31$ (CH_2OH^+) and $m/q = 18$ (H_2O^+) during heating at 2 K/s.

3.4. Coadsorption with Different Exposure Orders. To understand coadsorption experiments involving two or more species, it is important to explore whether the order or sequence of adsorption affects the results. If the system is in equilibrium, then the order of exposure should not matter. In short, reversing the order of exposure in our experiments does not affect the basic observation that water decreases the rate of $\text{CF}_3\text{CH}_2\text{OH}$ desorption while increasing the rate of $(\text{CF}_3\text{CF}_2)_2\text{O}$ desorption. Figure 8 shows TPD spectra of coadsorbed $\text{CF}_3\text{CH}_2\text{OH}$ and water adsorbed on the $\text{a-CH}_{\text{Quan}}$ surface at 100 K with different orders of exposure. Equivalent coverage TPD spectra of $\text{CF}_3\text{CH}_2\text{OH}$ and water adsorbed individually are also plotted for comparison. The water coverage was kept constant at 1.20 ± 0.01 ML and the $\text{CF}_3\text{CH}_2\text{OH}$ coverage was kept constant at 0.20 ± 0.02 ML. There are some differences between the desorption spectra of the $\text{CF}_3\text{CH}_2\text{OH}$ obtained with different exposure sequences. However, for both exposure sequences, it is evident at 160 K that the $\text{CF}_3\text{CH}_2\text{OH}$ desorption rate is lowered by the addition of 1.2 ML of water. This indicates that the desorption energy of $\text{CF}_3\text{CH}_2\text{OH}$ increases with water coverage irrespective of the order of exposure.

Coadsorption experiments in which the order of exposure to $(\text{CF}_3\text{CF}_2)_2\text{O}$ and water were reversed both reveal that coadsorbed water decreases the desorption energy of $(\text{CF}_3\text{CF}_2)_2\text{O}$. Figure 9 shows TPD spectra of coadsorbed $(\text{CF}_3\text{CF}_2)_2\text{O}$ and water with different orders of exposure and TPD spectra of $(\text{CF}_3\text{CF}_2)_2\text{O}$ and water adsorbed individually on the $\text{a-CH}_{\text{Quan}}$ surface at 100 K. The water coverage was kept constant at 0.24 ± 0.02 ML and the $(\text{CF}_3\text{CF}_2)_2\text{O}$ coverage was kept constant at 0.17 ± 0.01 ML. As in the case of coadsorbed $\text{CF}_3\text{CH}_2\text{OH}$ and water, there are some subtle differences between the spectra obtained with different orders of exposure and it is clear that the system is not fully equilibrated. However, at a

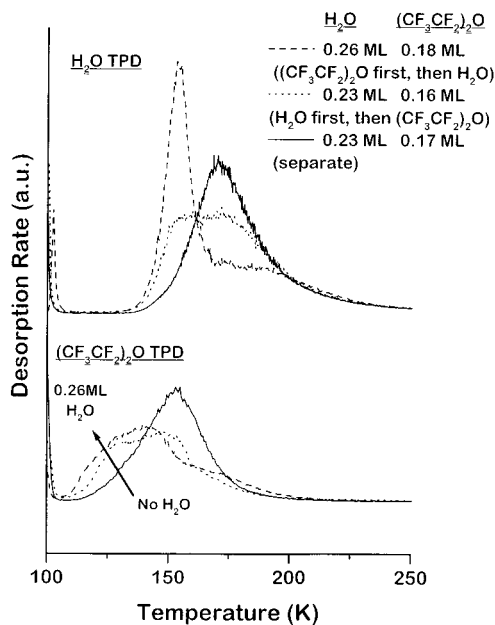


Figure 9. TPD spectra of coadsorbed $(\text{CF}_3\text{CF}_2)_2\text{O}$ and water with different orders of exposure and TPD spectra of $(\text{CF}_3\text{CF}_2)_2\text{O}$ and water adsorbed individually on an $\text{a-CH}_{\text{Quan}}$ surface at 100 K. Although the order of exposure influences the water and the $(\text{CF}_3\text{CF}_2)_2\text{O}$ TPD spectra, the presence of water always decreases the initial rate of desorption at the low-temperature leading edge of the $(\text{CF}_3\text{CF}_2)_2\text{O}$ spectrum. The water coverage was kept constant at 0.24 ± 0.02 ML. The $(\text{CF}_3\text{CF}_2)_2\text{O}$ coverage was kept constant at 0.17 ± 0.01 ML. The spectra were generated by simultaneously monitoring $m/q = 69$ (CF_3^+) and $m/q = 18$ (H_2O^+) during heating at 2 K/s.

low temperature (125 K) it is clear that the desorption rate of $(\text{CF}_3\text{CF}_2)_2\text{O}$ is increased by the coadsorption of 0.24 ML of water. Apparently the desorption energy of $(\text{CF}_3\text{CF}_2)_2\text{O}$ decreases with water coverage irrespective of the order of exposure.

4. Discussion

4.1. Interactions of $\text{CF}_3\text{CH}_2\text{OH}$, $(\text{CF}_3\text{CF}_2)_2\text{O}$, and Water with a-CH_x . The nature of the interaction of alcohols with amorphous nitrogenated carbon films (a-CN_x) was investigated by Paserba et al.²² and has also been investigated on a-CH_x films by Shukla et al.²⁷ A good measure of the hydrogen bond strength of $\text{CF}_3\text{CH}_2\text{OH}$ to the a-CH_x overcoat is the desorption energy (E_d) estimated using Redhead's equation.²⁸ The previous studies of alcohol adsorption on the a-CH_x and a-CN_x films showed that fluorination of the alcohols increased the desorption energy. They concluded that alcohols interact with the a-CH_x film through hydrogen bonding.^{22,27} Previous studies of the interaction of ethers with the a-CH_x overcoats showed that fluorination of the ether lowers their desorption energy. On this basis it was proposed that their interaction with the a-CH_x films occurs through a dative bond, formed via electron donation from the oxygen lone pair electrons to the amorphous film.^{15,22} The bonding mechanism of water to a-CH_x films is not very well understood. Perry et al.⁹ studied the adsorption of D_2O on a-CH_x films with different hydrogen content but did not attempt to reach a firm conclusion regarding the nature of the interaction. However, it is well-established that water acts as a Lewis base, an electron donor, in bonding to metal surfaces.^{25,29,30} Water may be bonded to the many acidic sites on the a-CH_x film in the same manner as a Lewis base.

(27) Shukla, N.; Gellman, A. J. To be published.

(28) Redhead, P. A. *Vacuum* **1962**, *12*, 203–211.

The desorption energies observed for $\text{CF}_3\text{CH}_2\text{OH}$, $(\text{CF}_3\text{CF}_2)_2\text{O}$, and water on a- CH_x films cover a broad range due to the heterogeneity of the a- CH_x film. In principle, a carbon atom can adopt three different electronic configurations: sp^3 , sp^2 and sp^1 . Graphite and diamond have pure sp^2 and sp^3 electronic configurations, respectively, and a- CH_x films have a mixture of both sp^2 and sp^3 bonded carbon atoms.³¹ This dual nature of the electronic structure of the carbon in a- CH_x films gives rise to its heterogeneity. At a finer level of detail, the carbon atoms can be coordinated in a number of different ways, including CCH_3 , C_2CH_2 , CC(H)=C , partially oxidized structures such as C=O , COH , and C-O-C groups, and carbon dangling bonds. It is not surprising that these films contain a variety of sites for molecular adsorption having a range of affinities for the adsorption of $\text{CF}_3\text{CH}_2\text{OH}$ and $(\text{CF}_3\text{CF}_2)_2\text{O}$.^{15,32} $\text{CF}_3\text{CH}_2\text{OH}$, $(\text{CF}_3\text{CF}_2)_2\text{O}$, and water bond to the sites for which they have the highest affinity or binding strength. The TPD spectra obtained at increasing coverages reveal that the desorption peak temperatures decrease with increasing coverage. The implication is that the various binding sites are populated sequentially from highest to lowest affinity as the coverage increases. It is the heterogeneity of the carbon films that is responsible for the coverage dependent peak desorption temperatures and the breadth of the desorption features at monolayer coverages, both of which are due to coverage dependent desorption energies.

It should be pointed out that a second potential source of coverage dependence in the desorption energy is the interaction between molecules on the surface as coverage increases. In the context of that model, the apparent decrease in the desorption energy with coverage would be interpreted in terms of a repulsive interaction between adsorbed molecules. However, this has been ruled out by experiments performed on the Cu(111) surface^{15–17} and on graphite,²⁷ both of which reveal weak attractive interactions between adsorbed $\text{CF}_3\text{CH}_2\text{OH}$ and between adsorbed $(\text{CF}_3\text{CF}_2)_2\text{O}$. As such, the coverage dependence of the desorption energy of these species on the a- CH_x films is attributed predominantly to the heterogeneity of the film surface.

Finally, having discussed the nature of the interactions of $\text{CF}_3\text{CH}_2\text{OH}$, $(\text{CF}_3\text{CF}_2)_2\text{O}$, and water with a- CH_x films, the focus of this work has been to address the nature of their intramolecular interactions when coadsorbed on these films. There are many possible mechanisms of water–lubricant interaction on an a- CH_x overcoat. First, water might react with the lubricant, or water might react with the overcoat itself and thus modify its interaction with the lubricant. However, there was no evidence of reaction observed in any of the TPD experiments conducted in this work. As a second mechanism for interaction, water might displace lubricant from the adsorption sites on the overcoat for which it has the greatest affinity. If water and $(\text{CF}_3\text{CF}_2)_2\text{O}$ were to compete for adsorption onto the same sites, water with greater desorption energy would displace $(\text{CF}_3\text{CF}_2)_2\text{O}$ from those sites, forcing it to adsorb to sites for which it has a lower binding affinity. The outcome of competition between water and $\text{CF}_3\text{CH}_2\text{OH}$ for binding sites is less clear, because they have roughly the same range of desorption energies. As a third

interaction mechanism, water and lubricant adsorbed on different sites might interact with each other through space. As mentioned, previous work on the very homogeneous Cu(111) and graphite surfaces has revealed that the natural interactions between adsorbed $\text{CF}_3\text{CH}_2\text{OH}$ and between adsorbed $(\text{CF}_3\text{CF}_2)_2\text{O}$ are attractive. The nature of the hetero-molecular interactions between water and these species are unclear.

4.2. Effect of Water on $(\text{CF}_3\text{CF}_2)_2\text{O}$ Bonding to a- CH_x . The desorption energy of $(\text{CF}_3\text{CF}_2)_2\text{O}$ on a- CH_x decreases with increasing water coverage. It is difficult to quantify this decrease in desorption energy because of the heterogeneity of the a- CH_x surface and the complexity of the TPD spectra. Instead of using the Redhead equation directly, we have chosen to analyze the desorption spectra qualitatively by examining their low-temperature leading edges. For a first-order desorption process, the desorption rate is equal to the product of the rate constant and coverage ($r = k\theta$). At the leading edge of the desorption curve the coverage remains roughly constant and desorption can be described as a pseudo-zero-order process. As such, the leading edge, which is a measure of the rate of desorption, is also a measure of the desorption rate constant at the initial coverage of adsorbate. This rate constant is predominantly determined by the desorption energy

$$k = \nu \exp\left(\frac{-E_d}{RT}\right)$$

Therefore, over the temperature range of the leading edge, the spectrum with the greatest desorption rate indicates desorption with the greatest rate constant (k) and hence the lowest desorption energy. Examining the leading edges of Figures 6 and 7 suggests that the desorption energy of $(\text{CF}_3\text{CF}_2)_2\text{O}$ decreases with increasing water coverage.

The coadsorption of water and $(\text{CF}_3\text{CF}_2)_2\text{O}$ has also been studied on other surfaces. Leavitt and Thiel²⁶ observed a decrease in desorption energy of $(\text{CF}_3\text{CF}_2)_2\text{O}$ when coadsorbed with water on the Ru(100) surface. They observed a 25 K decrease in the peak temperature of $(\text{CF}_3\text{CF}_2)_2\text{O}$ desorption, similar to that observed in Figures 6 and 7. They explained this behavior with Lewis acid–base theory. Water and $(\text{CF}_3\text{CF}_2)_2\text{O}$ are both Lewis bases or electron pair donors. Water is the stronger Lewis base, because the electron density in $(\text{CF}_3\text{CF}_2)_2\text{O}$ is more delocalized than in the compact water molecule. In the case of the Ru(100) surface with homogeneous binding sites, water, being the stronger base, donates electron density to the surface, making the formation of the $(\text{CF}_3\text{CF}_2)_2\text{O}$ dative bond to the surface weaker.

In our case, the a- CH_x surface has a variety of binding sites with a range of affinities for the adsorption of water and $(\text{CF}_3\text{CF}_2)_2\text{O}$. The increase in electron density of the a- CH_x surface when water is adsorbed will be more highly localized than on a metal surface and the through-surface interaction should have less influence on the $(\text{CF}_3\text{CF}_2)_2\text{O}$ desorption energy on a- CH_x than on Ru(100). On the other hand, if both $(\text{CF}_3\text{CF}_2)_2\text{O}$ and water adsorb by the same mechanism of electron donation, and the a- CH_x surface is heterogeneous, it is reasonable to suggest that they will compete for the same binding sites. Water, with the higher desorption energy, will adsorb preferentially to those sites with the greatest affinity for electron donors. As a result, $(\text{CF}_3\text{CF}_2)_2\text{O}$ will be displaced by the addition of water to lower affinity sites, resulting in a lower desorption energy. Figure 10 illustrates this displacement mechanism, where a $(\text{CF}_3\text{CF}_2)_2\text{O}$ molecule adsorbed on a high-affinity site

(29) Holloway, S.; Bennermann, K. H. *Surf. Sci.* **1980**, *101*, 327–333.

(30) Sexton, B. A. *Surf. Sci.* **1980**, *94*, 435–445.

(31) Robertson, J. *Adv. Phys.* **1986**, *35*, 317–374.

(32) Yanagisawa, M. *Adsorption of Perfluoro-Polyether on Carbon Surfaces*; STLE Special Publication SP-36: Park Ridge, IL, 1994; Vol. 9, pp 25–32.

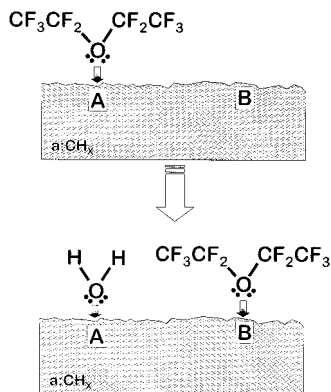


Figure 10. Proposed model for the displacement of $(\text{CF}_3\text{CF}_2)_2\text{O}$ on the a-CH_x surface by coadsorbed water. At low coverages the $(\text{CF}_3\text{CF}_2)_2\text{O}$ adsorbs preferentially on site "A" which has a higher affinity than site "B" for adsorption of $(\text{CF}_3\text{CF}_2)_2\text{O}$. In the presence of water, which has a higher desorption energy than $(\text{CF}_3\text{CF}_2)_2\text{O}$, the $(\text{CF}_3\text{CF}_2)_2\text{O}$ molecule adsorbed on the high-affinity site A is displaced to the low-affinity site B.

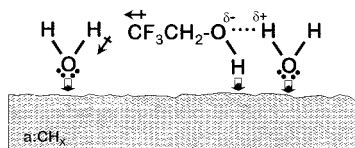


Figure 11. Possible models for the stabilization of adsorbed $\text{CF}_3\text{CH}_2\text{OH}$ on the a-CH_x surface by coadsorbed water. Water and $\text{CF}_3\text{CH}_2\text{OH}$ adsorbed on different sites could interact through a dipole-dipole interaction or a hydrogen-bond interaction.

"A" is displaced to a low-affinity site "B" by the adsorption of a water molecule at site A.

4.3. Effect of Water on $\text{CF}_3\text{CH}_2\text{OH}$ Bonding to a-CH_x . Examining the leading edges of the TPD spectra of Figures 4 and 5 shows that the rate constant for $\text{CF}_3\text{CH}_2\text{OH}$ desorption decreases with increasing water coverage. This suggests that there is an increase in the desorption energy of $\text{CF}_3\text{CH}_2\text{OH}$ on the $\text{a-CH}_{\text{Quan}}$ film. Since the desorption energies of water and $\text{CF}_3\text{CH}_2\text{OH}$ adsorbed individually on the a-CH_x film are approximately equal, the result of a competition for binding sites is unclear. The fact that they interact with the a-CH_x surface via different mechanisms (electron donation versus hydrogen bonding) makes it seem unlikely that there is competition between the two for the same binding sites. Furthermore, if there were competition for binding sites, it is hard to imagine how water would displace $\text{CF}_3\text{CH}_2\text{OH}$ onto sites for which it had higher affinity since it should naturally bind to those sites with or without the presence of coadsorbed water. Instead we propose that the effects of coadsorbed water on the adsorption of $\text{CF}_3\text{CH}_2\text{OH}$ are the result of intermolecular interactions which stabilize the adsorbed $\text{CF}_3\text{CH}_2\text{OH}$. There are many possible mechanisms that could explain this increase in desorption energy. It is important to point out that since we are only measuring desorption rates, it is only possible to propose interactions that are consistent with the observed effects of water on the desorption energies. There is no direct spectroscopic evidence to favor one mechanism over the other. Two possible mechanisms are depicted in Figure 11. In one, water and $\text{CF}_3\text{CH}_2\text{OH}$ adsorbed on different sites interact with each other through a dipole-dipole interaction that could stabilize the adsorbed $\text{CF}_3\text{CH}_2\text{OH}$. Another possibility is that water and $\text{CF}_3\text{CH}_2\text{OH}$ adsorbed on adjacent sites interact with each other through hydrogen bonding between the oxygen atom of the alcohol and the hydrogen atom of water.

Having made the above arguments describing the interactions of water and $\text{CF}_3\text{CH}_2\text{OH}$ on the $\text{a-CH}_{\text{Quan}}$ film, it is important to point out that this system is complicated and that the details of the surface chemistry are sensitive to the nature and origin of the film. The effect in which water increases the adsorption energy of $\text{CF}_3\text{CH}_2\text{OH}$ adsorbed on $\text{a-CH}_{\text{Seag}}$ overcoats was only observed for $\text{CF}_3\text{CH}_2\text{OH}$ coverages of <0.1 ML. The effect was not seen for higher coverages. The reason for this dependence on the source of the a-CH_x is unknown. Further investigation of the subject is planned using a-CH_x films deposited in situ. Using such virgin a-CH_x overcoats will provide results that are independent of air contamination due to atmospheric exposure.

4.4. Implications for Fomblin Zdol Interaction with a-CH_x . On a conventional computer hard disk, the a-CH_x overcoat and a thin layer of Fomblin Zdol are the only protection for the magnetic layer against head-disk contacts. It has been established that humidity plays an important role in the effectiveness of this protection system.^{7-13,21,26} In this investigation, we have determined that increasing humidity increases the desorption energy of $\text{CF}_3\text{CH}_2\text{OH}$, representative of the hydroxyl end groups of Fomblin Zdol, and decreases the desorption energy of $(\text{CF}_3\text{CF}_2)_2\text{O}$, representative of the ether-like linkages of the backbone of Fomblin Zdol. Since there are far more ether linkages than hydroxyl end groups per Zdol molecule, the results of our study imply that coadsorbed water produced by high humidity environments weakens the net interaction of the Fomblin Zdol with the a-CH_x overcoat. These weaker interactions are consistent with the higher molecular mobility of Fomblin Zdol observed in the presence of high humidity. Fomblin Zdol mobility is desired for lubricant replenishment in areas of the disk surface which have been depleted of lubricant by head-disk contact. However, lubricants with too great a mobility may be spun-off of the disk platter, decreasing the durability and lifetime of the hard disk.

5. Conclusion

TPD experiments performed after coadsorbing either $\text{CF}_3\text{CH}_2\text{OH}$ or $(\text{CF}_3\text{CF}_2)_2\text{O}$ with water on a-CH_x films have provided insight into the molecular interactions between water, Fomblin Zdol, and a-CH_x overcoats. These results show that water increases the strength of the interaction of $\text{CF}_3\text{CH}_2\text{OH}$ with the a-CH_x overcoat. This suggests possible interactions between water and $\text{CF}_3\text{CH}_2\text{OH}$ that stabilize its adsorption to the overcoat. Water weakens the interaction of $(\text{CF}_3\text{CF}_2)_2\text{O}$ with the a-CH_x overcoat, indicative of a displacement of $(\text{CF}_3\text{CF}_2)_2\text{O}$ to sites with lower affinity for adsorption of the $(\text{CF}_3\text{CF}_2)_2\text{O}$. The TPD spectra of these coadsorbed species showed some dependence on the order of exposure to the surface, suggesting that equilibrium was not completely achieved in the time frame of the experiments. Nonetheless, the basic result of strengthening $\text{CF}_3\text{CH}_2\text{OH}$ and weakening $(\text{CF}_3\text{CF}_2)_2\text{O}$ interaction with the surface is independent of the order of exposure. The implications of these results are that Fomblin Zdol should have higher mobility on the a-CH_x surface in the presence of high humidity.

Acknowledgment. This work was supported by the National Science Foundation under Grant #ECD-8907068. The government has certain rights to this material. In addition, the authors would like to thank Quantum Corp. and Seagate Corp. for supplying the a-CH_x surfaces used in this work. We would also like to thank Dr. Chris McFadden for discussions of the results.